Presented at the 21st European Photovoltaic Solar Energy Conference and Exhibition, Dresden, Germany, 4-8 September 2006

NEW HORIZONS IN III-V MULTIJUNCTION TERRESTRIAL CONCENTRATOR CELL RESEARCH

R. R. King, R. A. Sherif, D. C. Law, J. T. Yen, M. Haddad, C. M. Fetzer,
K. M. Edmondson, G. S. Kinsey, H. Yoon, M. Joshi, S. Mesropian,
H. L. Cotal, D. D. Krut, J. H. Ermer, and N. H. Karam
Spectrolab, Inc., 12500 Gladstone Ave., Sylmar, CA 91342 USA

ABSTRACT: The high efficiency of multijunction concentrator cells has the potential to revolutionize the cost structure of photovoltaic electricity generation, and still higher efficiencies can be reached. This paper discusses the dependence of 3- and 4-junction terrestrial concentrator cell efficiency on the bandgaps of their component subcells, based on theory and experiment. 4-junction cells limited by radiative recombination can reach over 58% in principle. Practical 4-junction cell efficiencies over 46% are possible with the right combination of bandgaps, taking into account series resistance and gridline shadowing, based on measured 39% 3-junction cell efficiency. Many of the optimum bandgaps for maximum energy conversion can be accessed with lattice-mismatched, or metamorphic semiconductor materials, and such cells have reached a new record efficiency of 39.3% (179 suns, AM1.5D, low-AOD, 25°C). The lower current and resulting lower I^2R resistive power loss in cells with 4 or more junctions is a particularly significant advantage in concentrator PV systems. The energy production of 3 to 6-junction cells with daily variation in air mass and spectrum is analyzed. Energy production is found to increase with each additional junction, due to reduced resistive power loss and better division of the solar spectrum over most of the day. Prototype 4-junction terrestrial concentrator cells have been grown by metal-organic vapor-phase epitaxy, with preliminary measured efficiency of 35.7% under the AM1.5 direct terrestrial solar spectrum at 256 suns.
Keywords: III-V Semiconductors, Concentrator Cells, High-Efficiency, Multijunction Solar Cell,
Gallium Arsenide Based Cells, Lattice-Mismatched, Metamorphic

1 INTRODUCTION

III-V multijunction solar cells under concentrated sunlight have demonstrated efficiency of 39.0% for lattice-matched cells [1]. 3-junction cells based on lattice-mismatched, or metamorphic (MM) materials have now reached a record 39.3% efficiency, independently confirmed under the terrestrial AM1.5D, low-AOD spectrum at 179 suns, the highest solar conversion efficiency for a photovoltaic device to date. The high efficiency of III-V multijunction concentrator cells, and the leverage it has on the cost per watt of all components of a concentrator photovoltaic system, have stimulated a dramatic expansion of research and commercial development of solar concentrator PV systems [2-7]. Even so, higher efficiencies are possible in the near future through changes in the subcell materials and multijunction cell architecture, which will lower the cost per watt of concentrator PV still further.

In this paper we first discuss the theoretical dependence of multijunction (MJ) cell efficiency on subcell bandgap in 3-junction (3J) and 4-junction (4J) terrestrial concentrator cells. The wavelength division of the solar spectrum in a multijunction cell can be made more efficient by the use of bandgaps accessible with lattice-mismatched materials, and by control of group-III sublattice disordering. 3- and 4-junction cell efficiencies achievable in practice are found by normalizing the ideal efficiencies to correspond to measured 39% efficiency in 3-junction cells. As the angle of the sun in the sky changes over the course of the day and the year, the air mass, incident spectrum, and current balance among subcells change as well. The impact of this effect on energy production is modeled for 3- to 6-junction solar cells. 4-junction terrestrial concentrator cells have been built, and experimental results are given for quantum efficiency and conversion efficiency under the AM1.5 direct terrestrial spectrum used for concentrators.

2 THEORETICAL AND PRACTICAL MULTIJUNCTION CELL EFFICIENCIES

A multijunction cell model has been developed to calculate efficiency under the terrestrial AM1.5 Direct (ASTM G173-03) solar spectrum, limited only by fundamental loss mechanisms. The dependence of 3-junction and 4-junction cell performance on the bandgaps of subcells 1, 2, and 3, is shown in a series of plots with iso-efficiency contours. One such chart is shown in Fig. 1, for ideal efficiency of 3-junction cells as a function of the subcell 1 (top subcell) bandgap E_{g1} and the subcell 2 bandgap E_{g2}, with the 3rd subcell bandgap E_{g3} held constant at 0.67 eV, the bandgap of germanium.

The basic principles used to calculate ideal efficiency of multijunction solar cells in this model are:

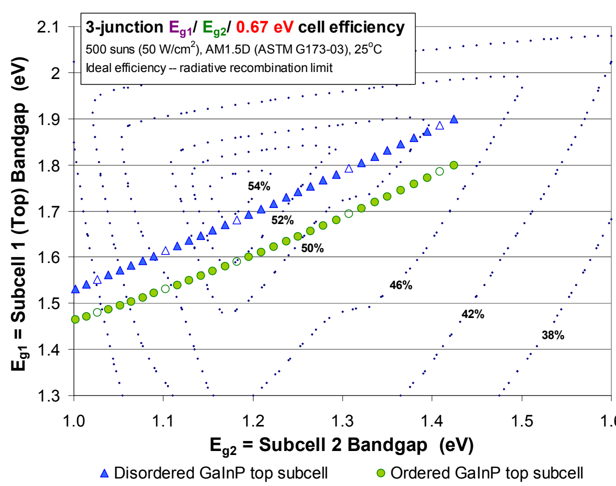

Figure 1: Contour plot of ideal efficiencies limited by radiative recombination, for 3-junction solar cells under the concentrated terrestrial solar spectrum at 500 suns.

1. Current density is based on the flux of photons available in the terrestrial solar spectrum above the bandgap energy of each subcell;

2. Open-circuit voltage and diode saturation current density are based on the fundamental mechanism of radiative recombination [1];

3. The multijunction cell light I-V curve is based on the diode characteristics of each series-interconnected subcell at the same current density;

4. The MJ cell design allows excess photogenerated current density in one subcell to be used by the cells beneath it to achieve current matching, within a specified subset of subcells.

The number of junctions in the cell is variable, with up to 10-junction solar cells easily accommodated by the model at present.

The recombination current density J_{rec} for radiative recombination is:

$$\begin{aligned} J_{rec} &= qwBpn = qwBn_i^2 e^{qV/kT} \\ &= J_o\left(e^{qV/kT} - 1\right) \approx J_o e^{qV/kT} \end{aligned} \tag{1}$$

for the case in which minority-carrier concentration is approximately constant across the solar cell base of thickness w, such that the diode saturation current density J_o of a solar cell limited by radiative recombination can be written:

$$J_o = qwBn_i^2 = qwBN_C N_V e^{-E_g/kT} \tag{2}$$

where B is the radiative recombination coefficient. To model solar cell efficiency as a function of subcell bandgap, the J_o must be found for the bandgap E_g of each subcell. By far the largest dependence of J_o on E_g arises from the exponential term in Eqn. 2. Different semiconductor materials can have significantly different values of N_C , the conduction band density of states. Materials with low density-of-states electron effective mass, such as InP, InAs, and perhaps ordered GaInP, can be expected to have lower N_C , and therefore lower J_o and higher V_{oc} than they would otherwise. In the model, the values and E_g dependences of B, N_C , and N_V were based on literature expressions and values, *e.g.*, references [8-10], but these dependences are not highly critical for establishing the general trends, because the strong exponential dependence of J_o on E_g dominates.

The subcell bandgaps needed to optimize the efficiency of cells with 3, 4, and more junctions are not always accessible with conventional semiconductors lattice-matched (LM) to common substrates like Ge, GaAs, InP, or Si. Lattice-mismatched, or metamorphic (MM) materials offer much greater flexibility of subcell bandgap selection for optimizing cell efficiencies, now up to 39.3%, provided that the increased recombination at dislocations in lattice-mismatched materials can be controlled [1-3,5]. The high lifetimes that have been achieved in metamorphic GaInAs and GaInP cells in spite of high lattice mismatch values of 1.6% and 2.4%, corresponding to 1.1-eV and 0.95-eV GaInAs bandgaps respectively [1], enable the use of more radical solar cell architectures such as inverted multijunction cells.

Bandgap combinations for a metamorphic GaInAs subcell 2 at various compositions, and a GaInP subcell 1 at the same lattice constant, are superimposed on the iso-efficiency contours in Fig. 1. The change in indium mole fraction in these MM materials allow different parts of the subcell bandgap space to be occupied, as does the degree of group-III sublattice disordering in the metamorphic GaInP top subcell. Both the cases of disordered (high E_g) and ordered (low E_g) group-III sublattice in metamorphic GaInP are plotted in Fig. 1.

Iso-efficiency plots for 2-junction cells have been presented in some very valuable articles in the literature, for example in [11] and others. In the time elapsed since those studies, the standard reporting spectrum for terrestrial concentrator cells has changed from the previous, red-rich AM1.5D ASTM E891-92 spectrum, to the AM1.5D low-AOD spectrum, which has now been adopted as the AM1.5D ASTM G173-03 spectrum. In addition to using this up-to-date standard spectrum, the 3- and 4-junction cell efficiency contour plots in this paper consider the optimum subcell bandgaps for these higher numbers of junctions. In order to be clear about which trends stem from fundamental physics and which result from real-life effects, separate contour plots are shown for ideal efficiency and for practical cell efficiency grounded in experimental cell measurements.

Figure 2 plots iso-efficiency contours where series resistance and grid shadowing have been taken into account, as well as other current, voltage, and fill factor losses, so that the calculated efficiency of a lattice-matched 3-junction GaInP/ GaInAs/ Ge cell corresponds to the experimental 39.0% 3J cell efficiency in [1], shown by the triangle in Fig. 2. This is referred to as the case normalized to measured 3J cell efficiency. Efficiencies of 41% can be seen to be practical in 3J cells with a 1.76/ 1.18/ 0.67 eV bandgap combination.

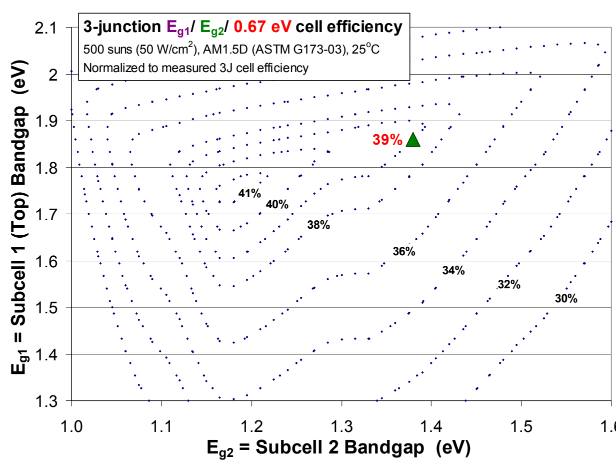

Figure 2: Contour plot of 3-junction cell efficiencies, including the effects of grid shadowing and series resistance, and normalized to correspond to the measured 39.0% efficiency for a 3-junction solar cell.

In Fig. 3, ideal efficiency and practical efficiency contours are plotted for 3-junction solar cells, this time as a function of the subcell 2 and subcell 3 (bottom subcell) bandgaps. The triangle again indicates the bandgap combination corresponding to measured 39% 3J cell efficiency. Ideal efficiencies of 53%, and practical efficiencies of 42%, are possible for 3-junction cells with a bandgap combination of 1.90/ 1.39/ 0.97 eV. These bandgaps can be accessed through the use of GaInP and GaInAs subcells 1 and 2 lattice matched to Ge or GaAs, and a metamorphic 0.97-eV GaInAs subcell grown inverted on a transparent graded buffer layer [1,5].

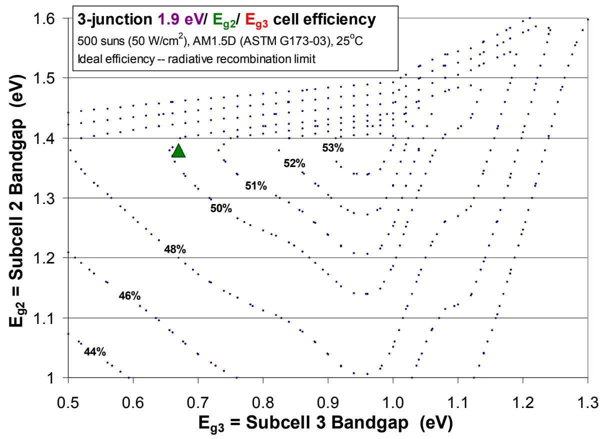

a.

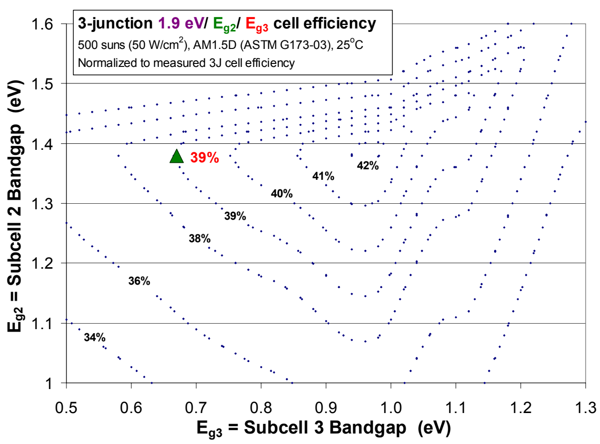

b.

Figure 3: Contour plots of a) ideal efficiency and b) efficiency normalized to experiment (39% measurement), for 3-junction cells under the 500X terrestrial spectrum, varying subcell 3 (bottom cell) and subcell 2 bandgaps.

A 4-junction (Al)GaInP/ AlGa(In)As/ Ga(In)As/ Ge terrestrial concentrator solar cell is shown in Fig. 4, where the parentheses indicate optional elements in the subcell composition. This type of cell divides the photon flux available in the terrestrial solar spectrum above the bandgap of the GaInAs subcell 3 into 3 pieces, rather than 2 pieces in the case of a 3-junction cell. As a result, the current density of a 4-junction cell is roughly 2/3 that of a corresponding 3-junction cell, and the I^2R resistive power loss is approximately $(2/3)^2 = 4/9$, or less than half that of a 3-junction cell.

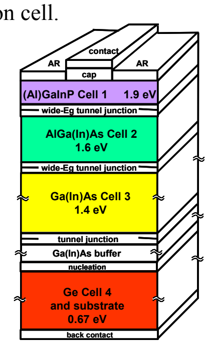

Figure 4: 4-junction AlGaInP/ AlGaInAs/ GaInAs/ Ge terrestrial concentrator solar cell cross section.

Iso-efficiency contours for 4-junction terrestrial concentrator cells, under the AM1.5D (ASTM G173-03) solar spectrum at 500X, are plotted in Fig. 5 as a function of the bandgaps of subcells 2 and 3. Ideal 4J cell efficiency is plotted in Fig. 5a, and practical cell efficiency, consistent with the measured efficiency of 39% for 3J cells, in Fig. 5b. The bandgap of subcell 1 is held at 1.9 eV, corresponding to GaInP at the Ge lattice constant with a disordered group-III sublattice, and subcell 4 (the bottom subcell) is fixed at the 0.67-eV bandgap of Ge, for this analysis.

The diamond in the plots indicates the 1.62/ 1.38 eV bandgap combination of the AlGaInAs subcell 2 and GaInAs subcell 3 of a 4-junction cell described later in the paper (see the quantum efficiency measurement in Fig. 9). Ideal efficiencies of over 58%, and practical cell efficiencies of 47% are possible for 4-junction terrestrial concentrator cells with a bandgap combination of 1.90/ 1.43/ 1.04/ 0.67 eV. It is worth noting that these practical 4J cell efficiencies are about 5 absolute efficiency points over those for 3-junction cells. 4-junction cells benefit from reduced resistive power losses as described above, and for this bandgap combination, more efficient use of the terrestrial solar spectrum.

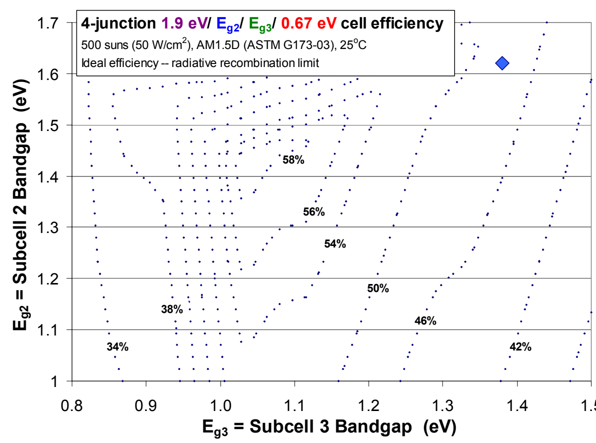

a.

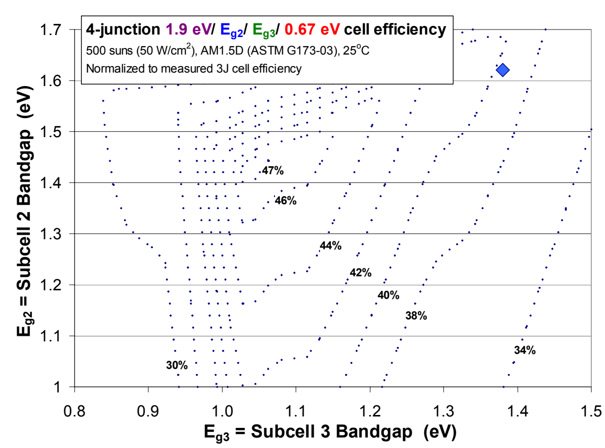

b.

Figure 5: Contour plots of a) ideal efficiency and b) efficiency normalized to experiment, for 4-junction solar cells, with variable subcell 3 and subcell 2 bandgaps.

3 ENERGY PRODUCTION

The variable angle of the sun causes a change in the air mass that sunlight must traverse before hitting the earth's surface, which tends to diminish the blue wavelengths of the solar spectrum more than longer wavelengths, as shown in Fig. 6. This results in a shift in current balance among the subcells between solar noon and the hours of the early morning or late afternoon.

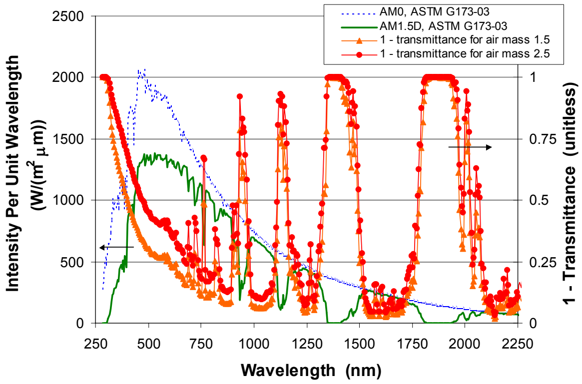

Figure 6: Attenuation of light intensity due to the atmosphere, for air mass 1.5 and 2.5.

When considering cells with 3, 4, 5, 6, or even more junctions under the shifting terrestrial solar spectrum, the question arises as to "which number of junctions is best for energy production over the day and year?" Energy production over the course of the day is calculated using ideal and practical efficiencies from the model described in the last section in order to answer this question. The calculations are for the autumnal equinox, to provide data for a typical day of the year, halfway between summer and winter.

The sun angle and air mass are calculated as a function of time on the autumnal equinox, and the terrestrial solar spectrum is calculated at 15 minute intervals based on the difference between the AM0 and the AM1.5D solar spectra in the ASTM G173-03 standard. Energy production is calculated for 3-, 4-, 5-, and 6-junction cells lattice-matched to Ge. Each type of MJ cell is first current balanced at a particular time of day, say at 12 noon or 3 PM (15:00 hours), by adjusting the bandgap of the subcells above the 1.4-eV GaInAs subcell. The cells can also be current balanced for a particular air mass by adjusting subcell thicknesses. The energy production is then calculated for that fixed cell design under each spectrum as a function of time of day.

Fig. 7 shows the energy production over the course of the day for 3-, 4-, 5-, and 6-junction cells, using practical cell efficiencies normalized to measured 3J cell efficiency. Each cell design was current balanced for the 1.75 air mass at 3 PM, near the optimum time of day for current balancing. The total intensity available in the solar spectrum as a function of time of day is also plotted for comparison, on a different axis. At extremely high air masses, the MJ cells with 4 and more junctions do have lower efficiency than 3-junction cells, but this has a negligible effect on total energy production for the day. For the vast majority of daylight hours, the energy production increases for each junction added to the MJ cell, for the MJ cell configurations in this study. This is due largely to the lower resistive power loss for cells with more junctions, and also to more efficient use of the solar spectrum. The increase in 4J cell energy production is substantially larger than for 3J cells, while the increase for 5J cells is smaller. The large difference between 5J cells and 6J cells is due to the inclusion of a 1-eV subcell 5 in the 6-junction case.

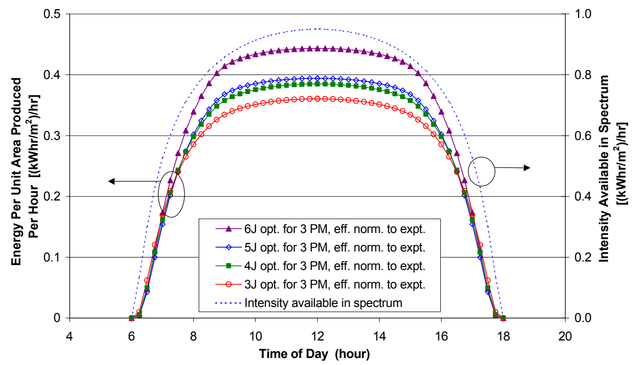

Figure 7. Energy production of multijunction cells with 3 to 6 junctions, with cell efficiency normalized to correspond to experimental values. Due largely to reduced series resistance losses, the energy production increases with each additional junction.

Figure 8 plots the energy produced per day for cells with 3 to 6 junctions, as a function of the time of day at which the MJ cell is current balanced. Current balance at 12 noon can be seen to be a local minimum for energy production, and the energy production is maximized if the cell is instead current balanced for the spectrum at 2:30-3:00 PM (or equivalently, 9:00-9:30 in the morning). The difference between current balancing at 12 noon and at the more optimal time later in the day becomes more pronounced with an increasing number of junctions. As before, the total energy generation per day is seen to increase with each added junction, in spite of concerns about current matching under variable air mass.

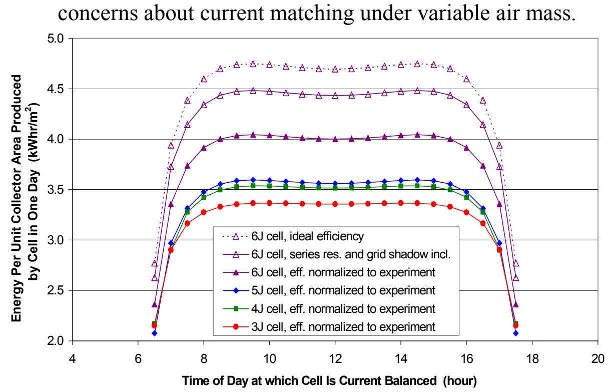

Figure 8. Energy production per day of terrestrial concentrator cells with 3 to 6 junctions, as a function of the time of day at which subcells are current balanced.

4 EXPERIMENTAL RESULTS

4-junction cells designed for the terrestrial solar spectrum and the high current densities of concentrator operation have been grown by metal-organic vapor-phase epitaxy (MOVPE), processed into devices, and tested. The external quantum efficiency of one such 4J cell is plotted in Fig. 9 versus photon energy. The bandgaps of each subcell can be determined from the quantum efficiency data, and the extracted values are listed in the legend. By convoluting with the terrestrial AM1.5D (ASTM G173-03) spectrum the current density of each subcell can also be determined. The current densities are 9.24, 9.24, 9.58, and 21.8 mA/cm2 for subcells 1, 2, 3, and 4, respectively, such that the subcells are very close to being current matched for this 4J cell.

Illuminated light I-V curves are shown in Fig. 10 for a 4-junction GaInP/ AlGaInAs/ GaInAs/ Ge solar cell measured at 256 suns, and for a similar solar cell with only the upper 3 junctions active (inactive Ge). The open-circuit voltage of the 4-junction cell is 4.364 V, compared to 3.960 V for the cell with an inactive subcell 4, indicating the the Ge bottom cell accounts for about 400 mV of the V_{oc} at this concentration. Independently confirmed measurements of a 39.0% lattice-matched cell [1], and a new record 39.3%-efficient metamorphic 3-junction cell (179 suns, AM1.5D, low-AOD, 25°C), are also shown. Preliminary measured efficiency for this still non-optimized 4J cell is 35.7% at 256 suns.

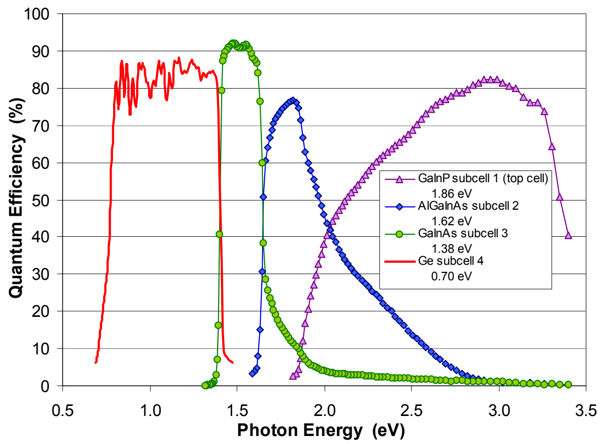

Figure 9. External quantum efficiency of a 4-junction GaInP/ AlGaInAs/ GaInAs/ Ge terrestrial conc. cell.

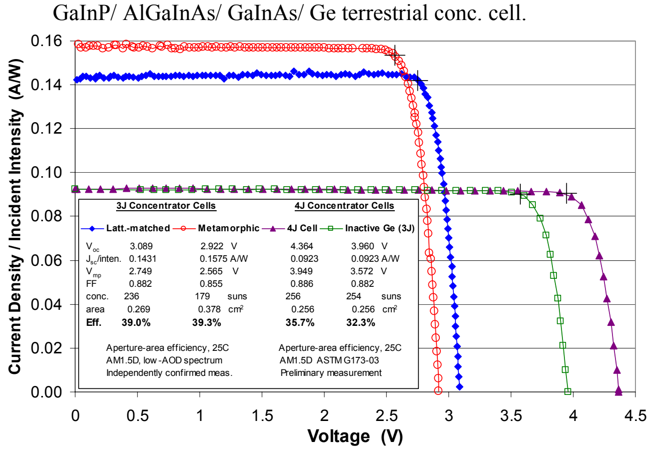

Figure 10. Illuminated I-V characteristics of an unoptimized 4-junction terrestrial concentrator cell with 35.7% efficiency, and V_{oc} over 4.3 volts. I-V curves for a 39.0% lattice-matched cell and a record 39.3%-efficient metamorphic 3-junction cell are also shown.

5 SUMMARY

The dependence of 3- and 4-junction terrestrial concentrator cell efficiency on the bandgaps of subcells 1, 2, and 3 is calculated, and presented in contour plots of both ideal efficiency and practical cell efficiency. Ideal cell efficiencies are over 58%, and practical efficiencies of 47% are achievable for 4-junction concentrator cells. The energy generation per day of cells with 4, 5, and 6 junctions is calculated, and found to be significantly higher than that of 3-junction solar cells, in spite of concerns about current matching under the variable solar spectrum. The low resistive power loss that results from the high-voltage, low-current design of cells with 4 or more junctions is a powerful advantage in concentrator applications. New 4-junction terrestrial concentrator cell architectures have been demonstrated, with 35.7% measured efficiency. Terrestrial concentrator cells with 3, 4, or more junctions, coupled with advances in metamorphic materials that have resulted in record solar cell efficiency of 39.3% today, offer the promise to increase efficiency and lower the cost of terrestrial photovoltaic concentrator systems still further.

6 ACKNOWLEDGMENTS

The authors would like to thank Robert McConnell, Martha Symko-Davies, Fannie Posey-Eddy, Keith Emery, James Kiehl, Tom Moriarty, Sarah Kurtz, Kent Barbour, Mark Takahashi, Andrey Masalykin, and the entire multijunction solar cell team at Spectrolab. This work was supported in part by the Dept. of Energy through the NREL High-Performance PV program (NAT-1-30620-01), and by Spectrolab.

7 REFERENCES

[1] R. R. King *et al.*, "Pathways to 40%-Efficient Concentrator Photovoltaics," *Proc. 20th European Photovoltaic Solar Energy Conf.*, Barcelona, Spain, 6-10 June 2005.

[2] F. Dimroth, U. Schubert, and A. W. Bett, "25.5% Efficient $Ga_{0.35}In_{0.65}P/Ga_{0.83}In_{0.17}As$ Tandem Solar Cells Grown on GaAs Substrates," *IEEE Electron Device Lett.*, 21, p. 209 (2000).

[3] R. R. King *et al.*, "Metamorphic GaInP/GaInAs/Ge Solar Cells," *Proc. 28th IEEE Photovoltaic Specialists Conf. (PVSC)*, Sep. 15-22, 2000, Anchorage, Alaska, pp. 982-985.

[4] T. Takamoto *et al.*, "Multijunction Solar Cell Technologies – High Efficiency, Radiation Resistance, and Concentrator Applications," *Proc. 3rd World Conf. on Photovoltaic Energy Conversion (WCPEC)*, Osaka, Japan, May 11-18, 2003, p. 581.

[5] M. W. Wanlass et al., "Lattice-Mismatched Approaches for High-Performance, III-V, Photovoltaic Energy Converters," *Proc. 31st IEEE PVSC*, Lake Buena Vista, Florida, Jan. 3-7, 2005, p. 530.

[6] A. Bett *et al.*, "FLATCON^{TM}-Modules: Technology and Characterisation," *Proc. 3rd WCPEC*, Osaka, Japan, May 11-18, 2003, p. 634.

[7] R. A. Sherif, R. R. King, N. H. Karam, and D. R. Lillington, "The Path to 1 GW of Concentrator Photovoltaics Using Multijunction Solar Cells," *Proc. 31st IEEE PVSC*, Lake Buena Vista, Florida, Jan. 3-7, 2005, p.17.

[8] R. K. Ahrenkiel, "Minority-Carrier Lifetime in III-V Semiconductors," Chap. 2, in *Semiconductors and Semimetals*, Vol. 39, Eds. R. K. Willardson, A. C. Beer, E. R. Weber (Academic Press, New York, 1993).

[9] R. N. Hall, *Proc. Inst. Elect. Eng.*, **106B**, Suppl. 17, 983 (1960).

[10] S. Adachi, *GaAs and Related Materials*, (World Scientific, River Edge, NJ, 1994).

[11] M. W. Wanlass *et al.*, "Advanced High-Efficiency Concentrator Tandem Solar Cells," *Proc. 22nd IEEE PVSC*, 1991, p. 38.